

Simplified Model of Dismount MicroDoppler and RCS

Dave Tahmoush

US Army Research Laboratory
2800 Powder Mill Rd, Adelphi, MD 20783

Jerry Silvious

US Army Research Laboratory
2800 Powder Mill Rd, Adelphi, MD 20783

Abstract—Our goal is to be able to detect and classify dismounts, but we were lacking a quick way to estimate dismount parameters, especially with respect to angle of motion and depression angle of the radar. Micro-Doppler models have been developed which attempt to predict the human micro-Doppler response, and here we present a simplified model to quickly estimate dismount RCS and some micro-Doppler characteristics across a range of angles of motion. This model was extracted from measured radar data. We focus on modeling and measuring the characteristics of human walking parameters to determine response of dismounts to radar signals. We determine a simple closed form for RCS as a function of angle for walking dismounts as well as several rules of thumb, and we also determine a closed form for front-view micro-Doppler.

I. INTRODUCTION

Detailed radar processing can reveal many characteristics of human motions and of the human body, including gait characteristics and radar-cross sections (RCS). Micro-Doppler signals refer to Doppler scattering returns produced by the motions of the target other than gross translation. These parts of the human body do not move with constant radial velocity; some of the small micro-Doppler signatures are periodic and therefore analysis techniques can be used to obtain more characteristics [1, 2]. Micro-Doppler gives rise to many detailed radar image features in addition to those associated with the bulk target motions. Modulations of the radar return from arms, legs, and even body sway are being investigated by researchers [3, 4, 5]. There are also some tutorials on micro-Doppler phenomena [2, 6, 7].

The equation for computing the non-relativistic Doppler frequency shift, F_d , of a simple point scatterer moving with speed v with respect to a stationary transmitter is

$$F_d = F_t \frac{2v}{c} \cos \theta \cos \phi \quad (1)$$

where F_t is the frequency of the transmitted signal, θ is the angle between the subject motion and the beam of the radar in the ground plane, ϕ is the elevation angle between the subject and the radar beam, and c is the speed of light. For complex objects, such as walking humans, the velocity of each body part varies over time. Additionally, the radar cross-section of various body parts is a function of aspect angle and

frequency. Ka-band frequencies have the potential to measure very fine details of the micro-Doppler spectrum [5].

Several micro-Doppler models have been developed which characterize and attempt to predict the human micro-Doppler response [8, 9, 10] and the underlying motion of different body parts is shown in Figure 1. Extraction of micro-Doppler features is typically performed in the joint time-frequency domain. Chirplet techniques can be used to perform feature extraction [5, 11] as well as linear FM basis decomposition [12]. Independent component analysis (ICA) can be used to extract independent basis functions from the spectrogram to be used as features in a classifier [13]. Micro-Doppler signatures have been suggested as a biometric [14], and micro-Doppler features have been used in classification algorithms [14, 15, 16, 17]. Micro-Doppler signatures and direction-of-arrival (DOA) estimates have been extracted at over nine meters range through a brick wall [18]. Fully polarimetric human radar signatures at different approach angles with respect to the radar have been collected [19]. Automatic target classification has also been done on data including multiple humans, wheeled vehicles, tracked vehicles, clutter, and animal classes [20].

The need for a simplified model of dismount RCS and micro-Doppler characteristics is for the development of systems to detect dismounts. Our model allows the calculation of relevant RCS and micro-Doppler parameters simply and easily in order to help evaluate and qualify dismount detection systems.

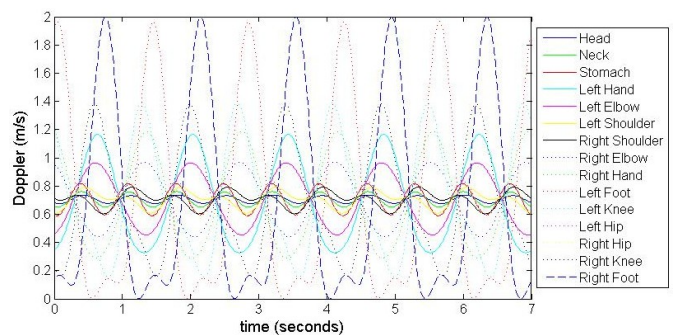


Fig. 1. Simulated Doppler motions for a man walking, with the Doppler of each part of the man displayed. This simulation is noiseless. Note that body-part interactions are eliminated from this plot, and this simulated motion in the radial direction to the radar.

Report Documentation Page			Form Approved OMB No. 0704-0188		
Public reporting burden for the collection of information is estimated to average 1 hour per response, including the time for reviewing instructions, searching existing data sources, gathering and maintaining the data needed, and completing and reviewing the collection of information. Send comments regarding this burden estimate or any other aspect of this collection of information, including suggestions for reducing this burden, to Washington Headquarters Services, Directorate for Information Operations and Reports, 1215 Jefferson Davis Highway, Suite 1204, Arlington VA 22202-4302. Respondents should be aware that notwithstanding any other provision of law, no person shall be subject to a penalty for failing to comply with a collection of information if it does not display a currently valid OMB control number.					
1. REPORT DATE MAY 2010		2. REPORT TYPE		3. DATES COVERED 00-00-2010 to 00-00-2010	
4. TITLE AND SUBTITLE Simplified Model of Dismount MicroDoppler and RCS			5a. CONTRACT NUMBER		
			5b. GRANT NUMBER		
			5c. PROGRAM ELEMENT NUMBER		
6. AUTHOR(S)			5d. PROJECT NUMBER		
			5e. TASK NUMBER		
			5f. WORK UNIT NUMBER		
7. PERFORMING ORGANIZATION NAME(S) AND ADDRESS(ES) Army Research Laboratory, 2800 Powder Mill Rd, Adelphi, MD, 20783			8. PERFORMING ORGANIZATION REPORT NUMBER		
9. SPONSORING/MONITORING AGENCY NAME(S) AND ADDRESS(ES)			10. SPONSOR/MONITOR'S ACRONYM(S)		
			11. SPONSOR/MONITOR'S REPORT NUMBER(S)		
12. DISTRIBUTION/AVAILABILITY STATEMENT Approved for public release; distribution unlimited					
13. SUPPLEMENTARY NOTES See also ADM002322. Presented at the 2010 IEEE International Radar Conference (9th) Held in Arlington, Virginia on 10-14 May 2010. Sponsored in part by the Navy.					
14. ABSTRACT Our goal is to be able to detect and classify dismounts but we were lacking a quick way to estimate dismount parameters, especially with respect to angle of motion and depression angle of the radar. Micro-Doppler models have been developed which attempt to predict the human micro-Doppler response, and here we present a simplified model to quickly estimate dismount RCS and some micro-Doppler characteristics across a range of angles of motion. This model was extracted from measured radar data. We focus on modeling and measuring the characteristics of human walking parameters to determine response of dismounts to radar signals. We determine a simple closed form for RCS as a function of angle for walking dismounts as well as several rules of thumb, and we also determine a closed form for front-view micro-Doppler.					
15. SUBJECT TERMS					
16. SECURITY CLASSIFICATION OF:			17. LIMITATION OF ABSTRACT Same as Report (SAR)	18. NUMBER OF PAGES 4	19a. NAME OF RESPONSIBLE PERSON
a. REPORT unclassified	b. ABSTRACT unclassified	c. THIS PAGE unclassified			

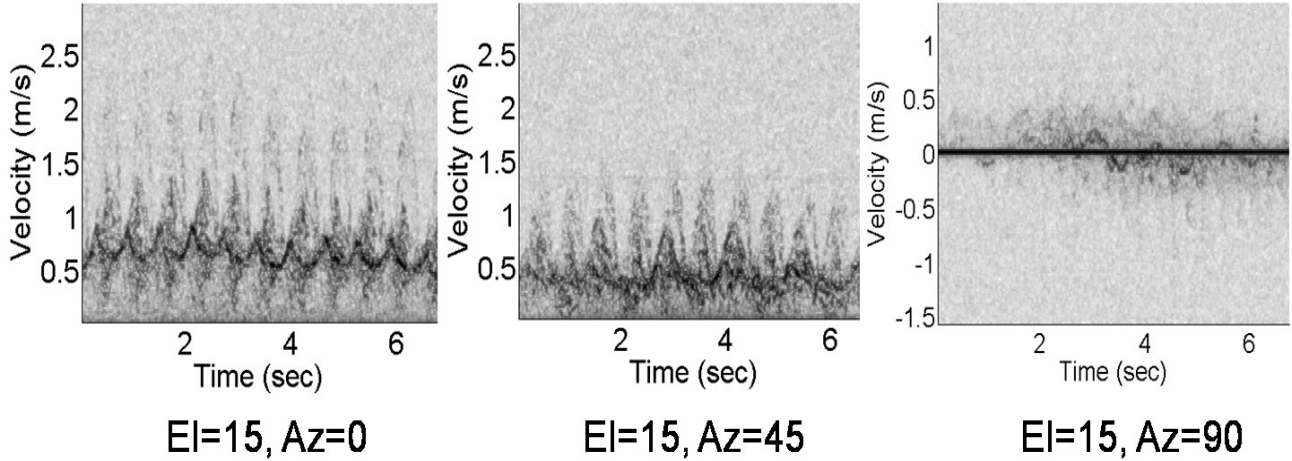


Fig 2. Doppler signature with azimuth angles of 0, 45, and 90 degrees. Note the change in average Doppler from 0.7 m/s to 0.5 m/s to 0 m/s. The Doppler is very difficult to see at 90 degrees due to clutter.

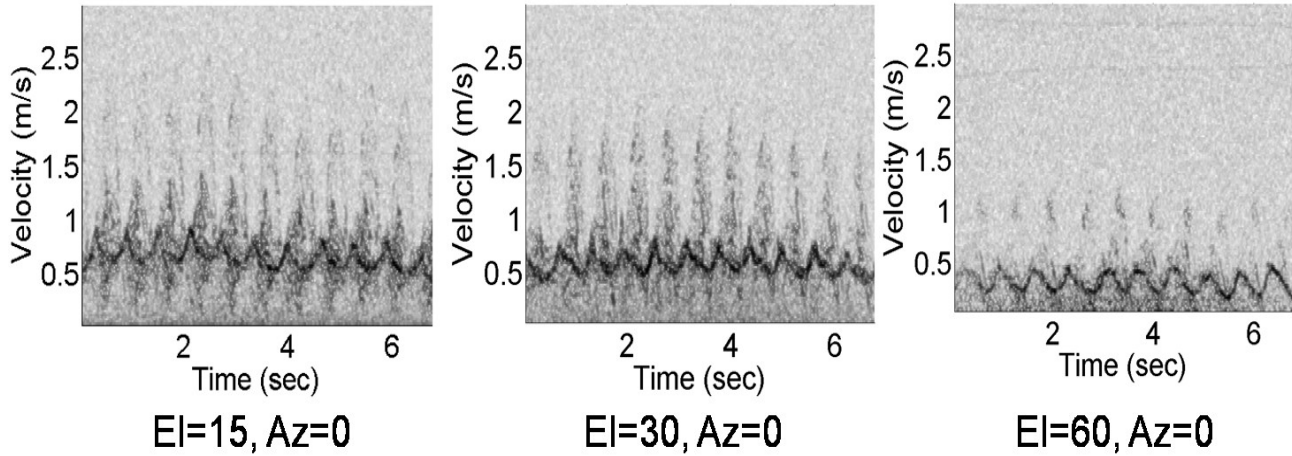


Fig 3. The variation of the Doppler signature with elevation at zero degrees azimuth, with the torso signature still visible at 60 degrees but with diminished amplitude.

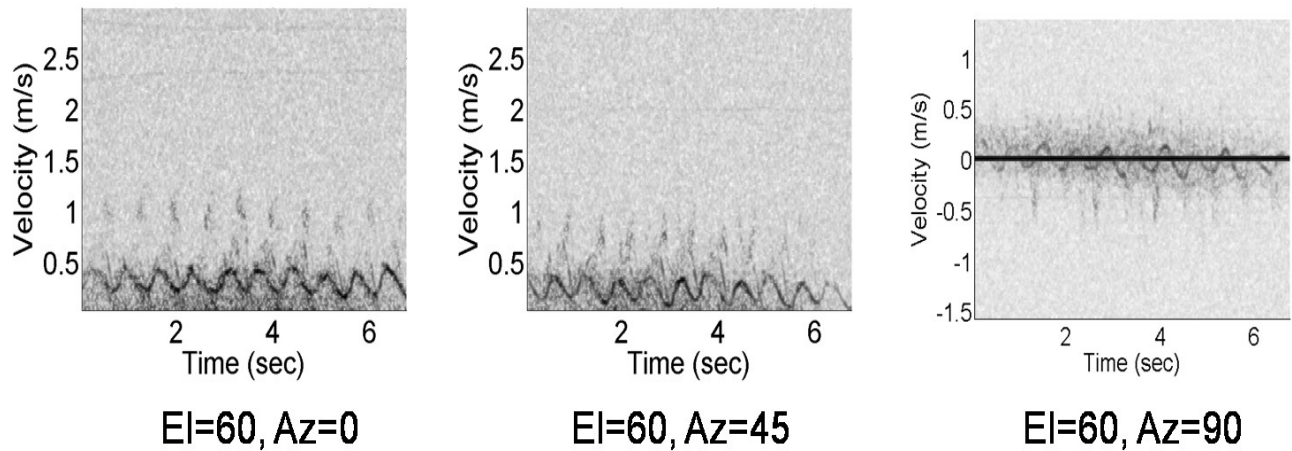


Fig 4. Doppler signature with azimuth angles of 0, 45, and 90 degrees but an elevation of 60 degrees. Note the Doppler can still be seen due to the elevation even though the azimuth angle is 90 degrees, but the negative velocities have to be kept.

II. CHARACTERIZING MEASUREMENTS

Multiple measurements were done to try to characterize the micro-Doppler of human motion. Measurements of humans were taken at the outdoor radar test range with realistic but

low levels of clutter. Measurements were done across a range of azimuth and elevation angles in order to characterize the micro-Doppler signature response of humans with respect to angle. The result of these experiments in azimuth is shown in

Figure 2. The measurement of the micro-Doppler is significantly more difficult as the motion approaches an angle that is perpendicular to the path of the radar illumination. This is because the relative Doppler is reduced by the angle of the motion relative to the path of the radar illumination. However, the side-to-side motion of human walking would show up [10].

The degradation of the micro-Doppler signature with elevation is not as severe, as can be seen in Figure 3. This is due to the coordinated rise and fall of the body with a walking motion. These results imply that coordinating the motion of people into the radar's field of view at zero elevation may not be necessary, since measurements with reduced but still viable signal levels can be made with a system that is at a higher elevation. Measurements at sixty degrees of elevation show measurable Doppler even at ninety degrees of azimuth, as shown in Figure 4. However, as the elevation increases, the offset from the zero velocity clutter line is diminished, making detection more challenging. This is especially true for measurements at ninety degrees of azimuth since the motion is centered at the clutter line.

III. SIMPLIFIED DOPPLER AND MICRODOPPLER

A simplified model for the mean torso velocity and for the micro-Doppler of walking dismounts is also helpful for determining the necessary system characteristics. The primary characteristics are the mean Doppler velocity and the size of the torso variation in the micro-Doppler. The mean torso velocity is found to vary along the lines of a simple scatterer, with a $\cos(\theta)\cos(\phi)$ dependence. However, the micro-Doppler is relatively consistent, with a 0.25 m/s peak to peak motion that is roughly sinusoidal, though interaction with the legs sharpens the point before the peak. It does not vary much with elevation, as can be seen in Figure 3. The azimuthal dependence is more complicated, with the motion being visible above 45 degrees of elevation at all azimuths, but being diminished or smeared at lower elevations and even moderate azimuth, as can be seen in Figure 2. The measurements angles were improved using simulated data as well, as can be seen in Figure 5. Several rules of thumb can be extracted for dismount torso velocity and micro-Doppler:

1. $\cos(\theta)\cos(\phi)$ dependence of average torso velocity
2. 0.25 m/s peak to peak micro-Doppler of the torso line roughly independent of elevation
3. Above 45 degrees of elevation, torso micro-Doppler is still visible

This model can be used to separate the micro-Doppler from the mean Doppler of the target, converting a complicated non-stationary signal into a simple scatterer. The simplified Doppler model is given in Equation 3.

$$\text{Doppler} = v \cos(\theta) \cos(\phi) + .25 \sin(\omega t + \tau) \quad (3)$$

where τ is the phase of the micro-Doppler motion. The ϕ dependence of the micro-Doppler term is not yet verified experimentally due to the complexity of the relationship. The residual differences have more to do with the inaccuracy of the torso extraction [21] than with the simplified model. One

thing to note is that the phase τ of the motion is often stable for more than four seconds for walking.

This model does work well for low elevations but not in combination with high azimuth. For true azimuthal dependence at low elevations of the micro-Doppler, simulations should be carried out. However, for quick calculations this model can still be used, allowing for a greater variability in the torso line, as can be seen by comparing Figures 2, 3, and 4. The torso line can be shadowed by the arm motion, as can be seen at 45 degrees in Figure 2. For example, the torso line appears at 5 seconds for about one half of a second as a strong dark line, then is shadowed for a second, and repeats earlier. Even at 90 degrees there appears to be some sinusoidal torso line for short periods.

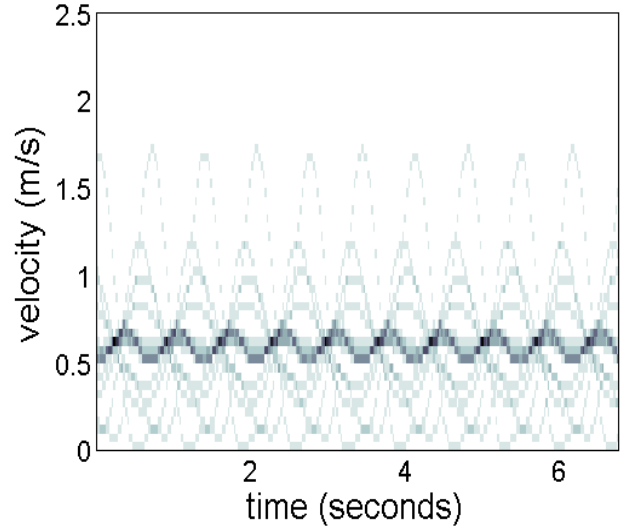


Fig 5. Simulated spectrogram of the motions in Figure 1. The motions of the separate parts of the body overlap and blur together, making extraction more difficult. Simulations were used to try to fill in angles in the measurements.

IV. RCS ESTIMATION

There are three different parameters that we allowed into the model for RCS. The first two are the angle θ , which is the angle between the subject motion and the beam of the radar in the ground plane, and the angle ϕ , which is the elevation angle between the subject and the radar beam. The third parameter in our RCS model is the number of dismounts in the same range gate. This is useful for estimating when you can see a large group moving together. The measurements are made with the clutter line subtracted, and the area was subjective, but the error was less than .5 dBc [19]. Note that the data is not highly sampled, so the resulting model must be simple.

The most inconsistent part of the model is the comparison of the RCS of a group of men. This falls roughly on the expected $-10\log_{10}(\text{number of dismounts})$ but can be inconsistent due to shadowing and other effects.

Incorporating the number of dismounts term, the remaining data can be combined together. The data on the dismounts at an elevation of 60 then shows very little variation with azimuth, primarily because the arm and leg motion is not as visible. This suggests a transition from multi-scatterer model to a single-scatterer model around an elevation of 45

degrees. The variation in RCS is then shown to roughly linearize as a function of $\cos^2(\phi)$ for both the 15 and 30 degree data.

Incorporating the azimuthal dependence with a cutoff at 45 degrees leaves only the elevation dependence to be determined. Using a least squares fit to the remainder of the data provides the final parameters to the model. The resulting RCS equation is then:

$$RCS = 6\cos^2(\varphi)H(\theta < 45) - 1.8\left(\frac{\theta}{15}\right) - 8 - 10\log_{10}N \quad (2)$$

where H is the Heaviside function defined to be one for θ less than 45 degrees and zero for θ greater than 45 degrees and N is the number of men in the group. Note, however, that the RCS measurements are at 35GHz and may not scale well to low frequencies. There is also some question as to how well the RCS can be measured at an azimuth of 90 degrees, where most of the signal is in the clutter line and the clutter cancellation is an issue. This simple equation encapsulates the drop in RCS with elevation as well as the strong azimuthal dependence at lower elevations. Several rules of thumb can then be extracted for dismount RCS:

1. Lose 1.8 dB per 15 degrees of elevation
2. Roughly lose 3 dB per 45 degrees in azimuth
3. Groups add like independent scatterers (often)

However, often the deciding factor is not just the RCS, but also the Doppler of the dismount in order to separate it from the clutter.

V. CONCLUSION

A simplified model for the RCS, the mean torso velocity, and for the micro-Doppler has been presented, along with several rules of thumb to help in the development of dismount detection. This model was extracted from measured radar data. We focus on modeling and measuring the characteristics of human walking parameters to determine response of dismounts to radar signals. We found that the mean torso velocity acts like a single moving scatterer with a $\cos(\theta)\cos(\phi)$ dependence on azimuth and elevation. We also found that the micro-Doppler of the torso line stays consistent at about 0.25 m/s peak to peak but it is strongly affected by azimuth when the elevation is less than 45 degrees. The micro-Doppler phase was also shown to be relatively stable over periods of a few seconds. For RCS, we determined that you lose 1.8 dB per 15 degrees of elevation, 3 dB per 45 degrees in azimuth, and that groups often add like independent scatterers.

ACKNOWLEDGMENT

The authors would like to thank Bob Tan.

REFERENCES

- [1] L. Cohen, *Time-Frequency Analysis*. Englewood Cliffs, NJ: Prentice-Hall, 1995.
- [2] V.C. Chen and H. Ling, *Time-frequency transforms for radar imaging and signal analysis*, Artech House, Norwood, MA, 2002.
- [3] S.Z. Gürbüz, W.L. Melvin, and D.B. Williams, "Detection and Identification of Human Targets in Radar Data," *Proc. SPIE Vol. 6567*, 2007.
- [4] Gene Greneker, "Very Low Cost Stand-Off Suicide Bomber Detection System Using Human Gait Analysis To Screen Potential Bomb Carrying Individuals," *Proc. SPIE Vol 5788*, 2005.
- [5] J.L. Geisheimer, W.S. Marshall, and E. Greneker, "A Continuous-Wave (CW) Radar for Gait Analysis," *Conference Record of the Thirty-Fifth Asilomar Conference on Signals, Systems and Computers*, 2001, Vol 1, pp. 834-838, Nov 2001.
- [6] V.C. Chen and R. Lipps, "Time frequency signatures of micro-Doppler phenomenon for feature extraction," *Proceedings of SPIE*, vol. 4056, *Wavelet Applications VII*, pp. 220-226, April 2000.
- [7] V.C. Chen, F. Li, S.-S. Ho, and H. Wechsler, "Micro-Doppler effect in radar: phenomenon, model, and simulation study," *IEEE Trans. on Aerospace and Electronic Systems*, vol. 42, pp. 2-21, January 2006.
- [8] D.A. Tahmouh and J. Silvius, "Radar MicroDoppler for Security Applications: Modeling Men versus Women," *Proceedings of the 2009 IEEE International Symposium on Antennas and Propagation*, Charleston, SC, 1-5 June, 2009.
- [9] P. van. Dorp and F.C.A. Groen, "Human walking estimation with radar," *IEEE Proc. on Radar, Sonar, and Navigation*, vol. 150, pp. 356-365, October 2003.
- [10] D.A. Tahmouh and J. Silvius, "Angle, Elevation, PRF, and Illumination in Radar MicroDoppler for Security Applications," *Proceedings of the 2009 IEEE International Symposium on Antennas and Propagation*, Charleston, SC, 1-5 June, 2009.
- [11] J. Li and H. Ling, "Application of adaptive chirplet representation for ISAR feature extraction from targets with rotating parts," *IEE Proc. on Radar, Sonar, and Navigation*, vol. 150, pp. 284-291, August 2003.
- [12] P. Setlur, M. Amin, and F. Ahmad, "Analysis of micro-Doppler signals using linear FM basis decomposition," *Proceedings of SPIE*, vol. 6210, *Radar Sensor Technology X*, May 2006.
- [13] V.C. Chen, "Spatial and temporal independent component analysis of micro-Doppler features," *IEEE Radar Conf.*, pp. 348-353, May 2005.
- [14] J.L. Geisheimer, E.F. Greneker, W.S. Marshall, "High-resolution Doppler model of the human gait," *Proc. SPIE 4744*, 8, 2002.
- [15] Y. Yang, J. Lei, W. Zhang, and C. Lu, "Target classification and pattern recognition using micro-Doppler radar signatures," *Seventh ACIS International Conference on Software Engineering, Artificial Intelligence, Networking, and Parallel/Distributed Computing*, 2006, pp. 213-217, June 2006.
- [16] P. Kealey and M. Jahangir, "Advances in Doppler recognition for ground moving target indication," *Proceedings of SPIE*, vol. 6234, *Automatic Target Recognition XVI*, May 2006.
- [17] M. Otero, "Application of a continuous wave radar for human gait recognition," *Proceedings of SPIE*, vol. 5809, *Signal Processing, Sensor Fusion, and Target Recognition XIV*, pp. 538-548, May 2005.
- [18] A. Lin and H. Ling, "Through-wall measurements of a Doppler and direction-of-arrival (DDOA) radar for tracking indoor movers," *IEEE Antennas Propagation Soc. Int. Symp. Digest*, vol. 3B, pp. 322-325, July 2005.
- [19] R. Tan and R. Bender, "Analysis of Doppler Measurements of People," *Targets and Backgrounds XII: Characterization and Representation*, edited by Wendell R. Watkins, Dieter Clement, *Proceedings of SPIE Vol. 6239*, 623908-1, 2006.
- [20] I. Bilik, J. Tabrikian, and A. Cohen, "GMM-based target classification for ground surveillance Doppler radar," *IEEE Transactions on Aerospace and Electronic Systems*, vol. 42, No. 1, pp. 267-278, January 2006.
- [21] D.A. Tahmouh and J. Silvius, "Radar Stride Rate Extraction," *Proceedings of the The 13th Irish Machine Vision and Image Processing conference (IMVIP 2009)*, Dublin, Ireland, Sept. 2009